Biosensors and Bioelectronics 47 (2013) 292–299

Contents lists available at SciVerse ScienceDirect

Biosensors and Bioelectronics

journal homepage: www.elsevier.com/locate/bios

Laccase–Prussian blue film–graphene doped carbon paste modified electrode for carbamate pesticides quantification

Thiago M.B.F. Oliveira [a,b], M. Fátima Barroso [a,c], Simone Morais [a,*], Mariana Araújo [d], Cristina Freire [d], Pedro de Lima-Neto [b], Adriana N. Correia [b], Maria B.P.P. Oliveira [c], Cristina Delerue-Matos [a]

[a] REQUIMTE, Instituto Superior de Engenharia do Porto, Instituto Politécnico do Porto, Rua Dr. Bernardino de Almeida 431, 4200-072 Porto, Portugal
[b] GELCORR, Departamento de Química Analítica e Físico-Química, Centro de Ciências, Universidade Federal do Ceará, Bloco 940, Campus do Pici, 60455-970 Fortaleza-CE, Brazil
[c] REQUIMTE, Departamento Ciências Químicas, Faculdade de Farmácia, Universidade do Porto, Rua de Jorge Viterbo Ferreira 228, 4050-313 Porto, Portugal
[d] REQUIMTE, Departamento de Química e Bioquímica, Faculdade de Ciências, Universidade do Porto, Rua do Campo Alegre s/n, 4169-007 Porto, Portugal

ARTICLE INFO

Article history:
Received 8 December 2012
Received in revised form
22 February 2013
Accepted 12 March 2013
Available online 21 March 2013

Keywords:
Enzymatic biosensors
Graphene
Prussian blue films
Laccase
Carbamates
Vegetables

ABSTRACT

A novel enzymatic biosensor for carbamate pesticides detection was developed through the direct immobilization of *Trametes versicolor* laccase on graphene doped carbon paste electrode functionalized with Prussian blue films (LACC/PB/GPE). Graphene was prepared by graphite sonication-assisted exfoliation and characterized by transmission electron microscopy and X-ray photoelectron spectroscopy. The Prussian blue film electrodeposited onto graphene doped carbon paste electrode allowed considerable reduction of the charge transfer resistance and of the capacitance of the device. The combined effects of pH, enzyme concentration and incubation time on biosensor response were optimized using a 2^3 full-factorial statistical design and response surface methodology. Based on the inhibition of laccase activity and using 4-aminophenol as redox mediator at pH 5.0, LACC/PB/GPE exhibited suitable characteristics in terms of sensitivity, intra- and inter-day repeatability (1.8–3.8% RSD), reproducibility (4.1 and 6.3% RSD), selectivity (13.2% bias at the higher interference:substrate ratios tested), accuracy and stability (*ca.* twenty days) for quantification of five carbamates widely applied on tomato and potato crops. The attained detection limits ranged between 5.2×10^{-9} mol L^{-1} (0.002 mg kg^{-1} w/w for ziram) and 1.0×10^{-7} mol L^{-1} (0.022 mg kg^{-1} w/w for carbofuran). Recovery values for the two tested spiking levels ranged from 90.2 ± 0.1 (carbofuran) to 101.1 ± 0.3% (ziram) for tomato and from 91.0 ± 0.1% (formetanate) to 100.8 ± 0.1% (ziram) for potato samples. The proposed methodology is appropriate to enable testing pesticide levels in food samples to fit with regulations and food inspections.

1. Introduction

Carbamate pesticides play an important role in high agriculture productivity (Dyk and Pletschke, 2011). Particularly in developing countries, these pesticides are systematically and increasingly applied as prophylactic measures due to their positive effect on yield (Oliveira et al., In press; Schwarzenbach et al., 2006). However, they are often toxic towards non-target organisms and their intentional release into the environment has been creating serious environmental and public health consequences worldwide. Carbamates are considered hazardous to human and environmental health, being included in the list of known endocrine disruptor compounds (Schulte-Oehlmann et al., 2011) and in the priority list released by the United States Environmental Protection Agency (USEPA, 2012a, 2012b). Therefore, monitoring of these pesticides in food and water is mandatory.

Pesticides usually inhibit various enzymes within insects and other pests leading to the incorporation of several classes of enzymes, mainly acetylcholinesterase and tyrosinase, into biosensors for detection purposes (Dyk and Pletschke, 2011). Laccase enzyme (LACC), a glycoprotein with four copper atoms per monomer distributed in three redox sites was successfully immobilized on some electrodic supports (Sabela et al., 2012; Durán et al., 2002). One of its main advantages as a recognition element is the covalently-linked carbohydrate moiety which may contribute to its high stability (Sabela et al., 2012). Despite its versatility as a recognition element on biosensors, the number of studies involving its application for pesticides determination is still very limited (Dyk and Pletschke, 2011; Morozova et al., 2007).

Carbon nanomaterials have been used as transducers to improve the electro-kinetic properties and sensitivity in the development of enzymatic biosensors, with a recent and important emphasis on

* Corresponding author. Tel.: +351 228340500; fax: +351 228321159.
E-mail address: sbm@isep.ipp.pt (S. Morais).

0956-5663/$ - see front matter © 2013 Elsevier B.V. All rights reserved.
http://dx.doi.org/10.1016/j.bios.2013.03.026

graphene (Kuila et al., 2011; Novoselov et al., 2004). Graphene-based electrodes have superior performance in terms of electrocatalytic activity and macroscopic scale conductivity than ones based on carbon nanotubes (Kuila et al., 2011; Jiang et al., 2011; Pumera et al., 2010; Novoselov et al., 2004). These unique properties are associated with the individual sheets, which are also responsible for its inherent disadvantages, such as hydrophobicity and easy aggregation in aqueous solution (Gu et al., 2012). They also exhibit high flexibility as a substrate for chemical and biological modifications (Bo et al., 2011; Shao et al., 2010). However, proper conjugation with biological molecules such as enzymes, ssDNA, RNA, Ab, receptors, and aptamers still needs to be further explored (Kuila et al., 2011; Shao et al., 2010). Furthermore, no direct application of graphene-based laccase biosensors was published for the detection of carbamate pesticides.

Studies have shown that the performance of carbon composite materials as transducers can be significantly enhanced upon modification with Prussian blue films (PB) (Jiang et al., 2011; Bo et al., 2011). PB behaves as an artificial peroxidase (Jiang et al., 2011; Bo et al., 2011), so when it is conjugated with a natural enzyme, the corresponding device acquires the characteristics of a bi-enzymatic system, greatly improving the biosensor performance (Fu et al., 2011; Li et al., 2008; Ricci and Palleschi, 2005).

In this work, a sensitive biosensor for carbamate pesticides detection was constructed, based on LACC immobilized directly on graphene doped carbon paste electrode (GPE), functionalized with PB. The optimal operational conditions (pH, enzyme concentration and incubation time) were determined using a 2^3 full-factorial statistical design and response surface methodology (RSM; Montgomery, 2005). The developed biosensor was applied to quantify a selection of carbamates used worldwide in tomato and potato crops, *i.e.*, carbofuran (CBF), carbaryl (CBR), formetanate (FMT), pirimicarb (PMB) and ziram (ZRM).

2. Experimental

2.1. Reagents

Spectroscopic grade graphite powder was purchased from Ultracarbon, (Spain). Laccase from *Trametes versicolor* (0.5 U mg^{-1}) and 4-aminophenol (4-AMP) were purchased from Sigma-Aldrich (Germany). The carbamates CBF, CBR, FMT, PMB, and ZRM were supplied from Fluka (Pestanal®, Germany). β-carotene (pro-vitamin A), tiamine (vitamin B1), ascorbic acid (vitamin C) and paraffin oil binder were obtained from Merck (Germany). D(+)-Glucose anhydrous was from Scharlau (Spain). Other chemicals were reagent grade and used without further purification.

Ultrapure water (ρ=18 MΩ cm^{-1}) was obtained by a Simplicity 185 apparatus (Millipore, Molsheim, France). A 0.04 mol L^{-1} Britton–Robinson (BR) buffer solution was employed for the testing of the biosensors.

Graphene was prepared by sonication-assisted exfoliation (Khan et al., 2011). 10 g of graphite powder was sonicated in 100 mL of N-methyl-2-pyrrolidone (Sigma-Aldrich) using a probe sonicator with a titanium tip (Bandelin Sonoplus) for 6 h. The dispersion was centrifuged at 500 rpm for 45 min; the supernatant containing the dispersed graphene flakes was removed and then filtered through a nylon 0.2 μm pore size membrane (Whatman). The resulting powder was dried by vacuum, at room temperature, for several days. Transmission electron microscopy (TEM) was performed with a Hitachi H-9000NA microscope operating at an accelerating voltage of 200–300 kV. The graphene sample was dispersed in high-purity ethanol under sonication, after which a carbon-coated 400 mesh copper grid was immersed in the suspension and then air-dried. X-ray photoelectron spectroscopy (XPS) was performed with a VG Scientific ESCALAB 200 A spectrometer using non-monochromatized Al Ka radiation (1486.6 eV). The powdered sample was pressed into pellets prior to the XPS studies. To correct possible deviations caused by electric charge of the samples, the C 1s band at 285.0 eV was taken as an internal standard. The XPS spectra were deconvoluted with the XPSPEAK 4.1 software, using non-linear least squares fitting routine after a Shirley-type background subtraction. The surface atomic percentages were calculated from the corresponding peak areas and by using sensitivity factors.

2.2. Electrochemical assays

Cyclic voltammetry (CV), square-wave voltammetry (SWV) and electrochemical impedance spectroscopy (EIS) were performed using an electrochemical system AutolabPGSTAT-30 (Eco Chemie, The Netherlands) and GPES/FRA software. The electrochemical cell was assembled with the developed enzymatic biosensor as the working electrode, a Ag/AgCl/KCl (3.0 mol L^{-1}) reference electrode, and a platinum counter electrode.

Optimization of the analytical procedure was performed using 4.75×10^{-5} mol L^{-1} 4-AMP as the redox mediator in BR buffer (pH 5.0), over the potential range from −0.4 to 1.4 V. EIS experiments were performed using a frequency range from 10^5 to 10^{-1} Hz with an amplitude perturbation of 5 mV, applying 0.20 (in the absence of LACC) and −0.01 V (in the presence of LACC) and using a 4.75×10^{-5} mol L^{-1} 4-AMP solution as the redox mediator.

2.3. Biosensor construction

A carbon paste was prepared by mixing spectroscopic grade graphite powder with a paraffin oil binder (70:30%, w/w) and carefully hand-mixing in a mortar and pestle. Subsequently, this paste was doped with different proportions of graphene (0, 10, 15, 20, 25 and 30%, w/w). The graphene doped carbon paste electrode (GPE) was packed into a handmade cavity of a Teflon® tube (1.0 mm internal diameter) and then provided by a stainless steel piston. The surface was smoothed against a plain white paper and rinsed with ultrapure water prior to each measurement.

The electrodeposition of PB films was carried out from an aqueous solution A (2 mmol L^{-1} $FeCl_3$, 2 mmol L^{-1} $K_3[Fe(CN)_6]$, 0.1 mol L^{-1} KCl and 0.1 mol L^{-1} HCl), applying a constant potential of +0.4 V (*vs.* Ag/AgCl) for different deposition times (5–40 s). Then, the modified electrode was washed with ultrapure water and transferred into the solution B (0.1 mol L^{-1} KCl and 0.1 mol L^{-1} HCl), and cycled twenty times between +0.05 and +0.35 V at a scan rate of 40 mV s^{-1}. After the activation, the probe denoted as PB/GPE was washed with water and dried with nitrogen (99.99% from LINDE, Portugal).

The LACC/PB/GPE biosensor was obtained by drop coating of LACC solution (5.0 to 15.0 U mL^{-1}) onto the PB/GPE surface and dried at room temperature. The biosensor construction was evaluated based on the intensity of background/faradaic currents, easy renewal of the surface and handling.

2.4. Optimization of the LACC/PB/GPE experimental parameters

Considering that the inhibition and catalytic process of LACC is directly related to the pH (X_1), enzyme concentration (X_2) and incubation time (X_3), and that synergistic effects between these variables can occur, operational conditions were optimized by a 2^3 full-factorial central composite design (CCD) and RSM (Montgomery, 2005). The CCD consisted of a complete factorial design (*i*), a central point (n_0, $n_0 > 1$, *ii*), and two axial points on the axis of each variable (*iii*) at a distance of α=1.682 from the center (Table 1). The full combination was composed of 20 experiments including 6 replicates

Table 1
Central composite design, observed and predicted peak currents, and ANOVA results obtained with LACC/PB/GPE in 4.75×10^{-5} mol L^{-1} 4-AMP (0.04 mol L^{-1} Britton–Robinson buffer, pH 5). Square-wave voltammetric conditions: frequency 100 s^{-1}, pulse amplitude 50 mV and scan increment 2 mV.

Experiment	Code and experimental values			Peak current (A)	
	$[X_1]$ [a]	$[X_2]$ [b]	$[X_3]$ [c]	Observed ± SD	Predicted
1	(−1) 4.5	(−1) 7.5	(−1) 10	$2.66 \times 10^{-7} \pm 3.51 \times 10^{-9}$	2.56×10^{-7}
2	(+1) 5.5	(−1) 7.5	(−1) 10	$2.88 \times 10^{-7} \pm 6.11 \times 10^{-9}$	2.68×10^{-7}
3	(−1) 4.5	(+1) 12.5	(−1) 10	$3.39 \times 10^{-7} \pm 4.00 \times 10^{-9}$	3.45×10^{-7}
4	(+1) 5.5	(+1) 12.5	(−1) 10	$4.67 \times 10^{-7} \pm 9.71 \times 10^{-9}$	4.63×10^{-7}
5	(−1) 4.5	(−1) 7.5	(+1) 20	$2.70 \times 10^{-7} \pm 5.03 \times 10^{-9}$	2.59×10^{-7}
6	(+1) 5.5	(−1) 7.5	(+1) 20	$4.24 \times 10^{-7} \pm 1.40 \times 10^{-9}$	4.28×10^{-7}
7	(−1) 4.5	(+1) 12.5	(+1) 20	$6.79 \times 10^{-7} \pm 8.00 \times 10^{-9}$	6.63×10^{-7}
8	(+1) 5.5	(+1) 12.5	(+1) 20	$7.22 \times 10^{-7} \pm 1.25 \times 10^{-9}$	7.15×10^{-7}
9	(−1.682) 4	(0) 10	(0) 15	$3.80 \times 10^{-7} \pm 8.33 \times 10^{-9}$	3.88×10^{-7}
10	(+1.682) 6	(0) 10	(0) 15	$7.87 \times 10^{-7} \pm 1.01 \times 10^{-9}$	7.95×10^{-7}
11	(0) 5	(−1.682) 5	(0) 15	$8.64 \times 10^{-7} \pm 1.02 \times 10^{-9}$	8.55×10^{-7}
12	(0) 5	(+1.682) 15	(0) 15	$7.43 \times 10^{-7} \pm 9.71 \times 10^{-9}$	7.58×10^{-7}
13	(0) 5	(0) 10	(−1.682) 5	$5.12 \times 10^{-7} \pm 5.51 \times 10^{-9}$	5.04×10^{-7}
14	(0) 5	(0) 10	(+1.682) 25	$1.75 \times 10^{-6} \pm 4.73 \times 10^{-8}$	1.63×10^{-6}
15	(0) 5	(0) 10	(0) 15	$1.77 \times 10^{-6} \pm 5.29 \times 10^{-8}$	1.92×10^{-6}
16	(0) 5	(0) 10	(0) 15	$2.17 \times 10^{-6} \pm 6.03 \times 10^{-8}$	1.92×10^{-6}
17	(0) 5	(0) 10	(0) 15	$1.85 \times 10^{-6} \pm 2.51 \times 10^{-8}$	1.92×10^{-6}
18	(0) 5	(0) 10	(0) 15	$1.85 \times 10^{-6} \pm 7.51 \times 10^{-8}$	1.92×10^{-6}
19	(0) 5	(0) 10	(0) 15	$1.91 \times 10^{-6} \pm 3.51 \times 10^{-8}$	1.92×10^{-6}
20	(0) 5	(0) 10	(0) 15	$1.76 \times 10^{-6} \pm 3.53 \times 10^{-8}$	1.92×10^{-6}

ANOVA regression model

Source	SS [d]	DF [e]	MS [f]	*F*-value	*p*
Model	8.31×10^{-12}	9	9.24×10^{-13}	6.102	0.0019
Residual	1.97×10^{-12}	13	1.51×10^{-13}	–	–
Lack of fit	1.95×10^{-12}	5	3.91×10^{-13}	224.0	< 0.001
Pure error	1.4×10^{-4}	8	1.74×10^{-5}	529.6	4.00×10^{-10}
Total (Model + residual)	1.03×10^{-11}	22	–	–	–
R^2	0.8086	–	–	–	–

[a] pH.
[b] Enzyme concentration (U mL^{-1}).
[c] Incubation time (minutes).
[d] Sum of squares.
[e] Degree of freedom.
[f] Mean square.

of the central point. The experimental domains (4–6 for pH, 5–15 U mL^{-1} for enzyme concentration and 5–25 min. for incubation time) were defined taking into account the results obtained in preliminary tests. The peak current (A) of 4.75×10^{-5} mol L^{-1} 4-AMP was taken as the dependent variable. Experimental data from the CCD were analyzed using RSM regression and fitted to a second-order polynomial model

$$y = \beta_0 + \sum_{i=1}^{k} \beta_i x_i + \sum_{i=1}^{k} \beta_{ii} x_i^2 + \cdots + \sum_{i}\sum_{i<j}\sum_{j} \beta_{ij} x_i x_j + \varepsilon. \quad (1)$$

where Y is the peak current (A) obtained for each condition, β_0 is the constant coefficient, β_i is the linear coefficient, β_{ii} is the coefficient of the squared effect and ε is the error of the model (Montgomery, 2005; Kondapalli et al., 2012, Sousa et al., 2012).

All statistical analyses were made using the software Statistica version 8.0 (StatSoft, Inc., Tulsa, UK). The two factors not represented by the horizontal axes in RSM plots were fixed at their 0 level values. Mean square residual was the error term chosen in all ANOVA tests of statistical significance.

2.5. Carbamate pesticides quantification

The selected carbamate pesticides were quantified based on the inhibition of the catalytic reaction of the redox mediator 4.75×10^{-5} mol L^{-1} 4-AMP (0.04 mol L^{-1}Britton–Robinson at pH 5) performed by LACC immobilized onto PB/GPE. The inhibition percentage (IR, %) of the 4-AMP analytical peak at −0.05 V and the concentration of the carbamates were employed to obtain analytical data (Miller and Miller, 2005).

2.6. Application to vegetable samples

Vegetable samples were obtained from local markets (Oporto region, Portugal). Samples of tomato and potato were taken, chopped and homogenized in accordance with guidelines of the European Council Directive (2002). The Quick, Easy, Cheap, Effective, Rugged and Safe—QuEChERS method (Paíga et al., 2012; Anastassiades et al., 2003) was selected for the extraction step. Briefly, an aliquot of 10 ± 0.05 g of homogenized sample was transferred to a tube containing the buffer–salt mixture 6 g $MgSO_4$/1.5 g NaCl/1.5 g $C_6H_5Na_3O_7.2H_2O$ (UCT, Bristol, USA). Next, 10 mL of acetonitrile were added and the QuEChERS tube was shaken vigorously during 1 min. After centrifugation in a 2.16 Sartorius centrifuge (Sigma, Goettingen, Germany), for 3 min at 4000 rpm, the solvent layer was evaporated under vacuum in a Büchi B-940 rotary evaporator (Büchi, Switzerland), and then with a gentle stream of nitrogen to complete dryness. Immediately before electroanalysis, the residue was re-dissolved with 10 mL of the supporting electrolyte (4.75×10^{-5} mol L^{-1} 4-AMP, 0.04 mol L^{-1} BR buffer solution at pH 5). Validation of the pesticide residue methodology was performed by recovery assays of fortified chopped and homogenized samples of tomato and potato, at two spiking levels using the standard additions method. All measurements were performed in triplicate.

3. Results and discussion

3.1. Graphene characterization

TEM micrographs of graphene (Fig. 1) confirm the effectiveness of the graphite exfoliation in N-methyl-2-pyrrolidone since graphene flakes with few layers are observed. As it is shown in Fig. 1A, the shape of the flakes is irregular, as well as the size; the length of the flakes varies from ~500 nm to ~1.5 μm. In the micrographs acquired at a major level of magnification (Fig. 1B), flakes with different thicknesses are observed. The surface atomic contents of graphene were determined by XPS as being 87.0% carbon, 12.4% oxygen and 0.5% nitrogen; these values indicate some degree of graphene oxidation and a small contamination with N-methyl-2-pyrrolidone used in the exfoliation process.

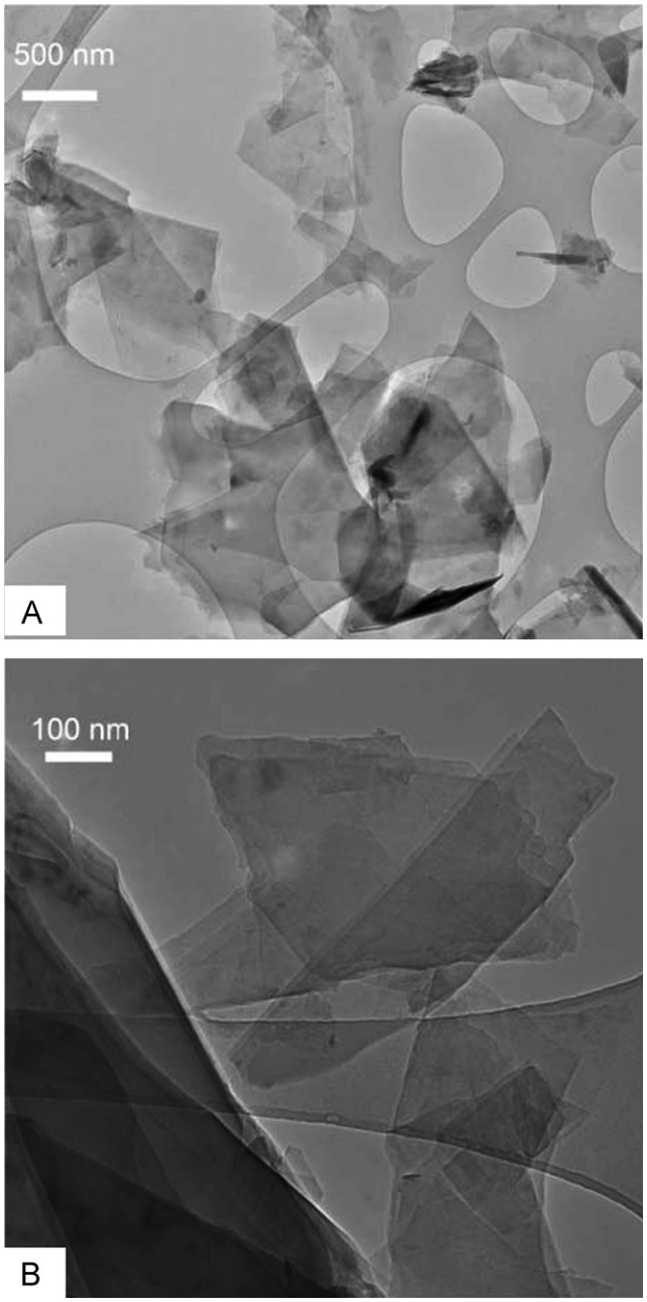

Fig. 1. TEM micrographs of graphene flakes obtained by sonication-assisted exfoliation of graphite in N-methyl-2-pyrrolidone showing irregular shape, size and length of the flakes (A), and different thickness at the major level of magnification (B).

3.2. Biosensor construction

3.2.1. Composition of the graphene doped carbon paste electrode

In order to investigate the best composition for the GPE (results not shown), different proportions of graphene (0, 10, 15, 20, 25 and 30%, w/w) mixed with prepared spectroscopic graphite powder paste (70:30%, w/w, grade graphite powder and paraffin oil binder) were evaluated by CV for a potential range from –0.2 to 0.6 V at a scan rate of 50 mV s^{-1}. In the absence of graphene, anodic and cathodic well-defined peaks, due to the redox pair of 4-AMP, were observed at +0.40 and +0.05 V, respectively. These peaks are related to the formation of a quinone–imine intermediate, which is represented by a quasi-reversible couple involving 2 H^+ and 2e^- (Salavagione et al., 2004). The presence of the graphene sheets in the composition of the paste allowed significant improvements in reversibility (anodic and cathodic peaks at +0.26 and +0.14 V, respectively), smallest separation of the peak potentials (ΔE_p), increase of the peak currents (I_p), and originated considerable catalytic effect of the redox processes. These data suggested that the doping of the composite material with graphene reduced the charge transfer resistance, and therefore originated a more interesting transducer. Considering that the highest peaks were observed with GPE containing 20% graphene (w/w) (approximately four times greater than that observed in the absence of graphene), this proportion was selected as optimum for the development of the enzymatic biosensor.

3.2.2. Electrodeposition and activation of the Prussian blue films

Based on previous reports (Jiang et al., 2011; Bo et al., 2011; Xue et al., 2006) mentioning that inorganic films are excellent supports for charge transfer in electrochemical sensors, the combination of PB and GPE was tested. The electrodeposition process was observed for scanning from –0.2 to 1.2 V (results not shown); two characteristic redox pairs appeared at the formal potentials of +0.20 V and +0.89 V (corresponding to the reduction of PB to Prussian white ($K_4Fe(II)_4[Fe(II)(CN)_6]_3$) and oxidation of PB to Berlin green ($Fe(III)_4[Fe(III)(CN)_6]_3Cl_3$), respectively) indicating the effective presence of PB on the GPE (Jiang et al., 2011).

Different PB electrodeposition times were investigated (Fig. 2A). Sharp anodic and cathodic peaks were observed, which are typical of a regular polycrystalline inorganic structure of the electrodeposited PB film; waveforms with $\Delta E_p \approx 60$ mV also suggested fast electrochemistry of the mono-electronic system for the active PB film (Jiang et al., 2011; Xue et al., 2006). Moreover, probably due to the high adsorptive characteristics of the composite material, good surface coverage of GPE was attained with just 5 s of electrodeposition, as observed by the well-defined obtained peaks (Fig. 2 A). The increase in the deposition time provided a linear increase of Ip_a and Ip_c until 20 s (inset of the Fig. 2A). CV data exhibited a linear relationship between the peak currents and the square root of the scan rate, for a range from 10 to 200 mV s^{-1}, indicating a diffusion-limited process (Maia et al., 2012). Nyquist plots (Fig. 2B) show a significant increase of the charge transfer resistance (R_{et}) with the increase of the deposition time, which can be associated with the increase of the PB layer thickness. Considering the acceptable capacitance for the film obtained with 15 s (R_{et} = 356 Ω), good stability, and short electrodeposition time, a period of 15 s was selected for the further experiments.

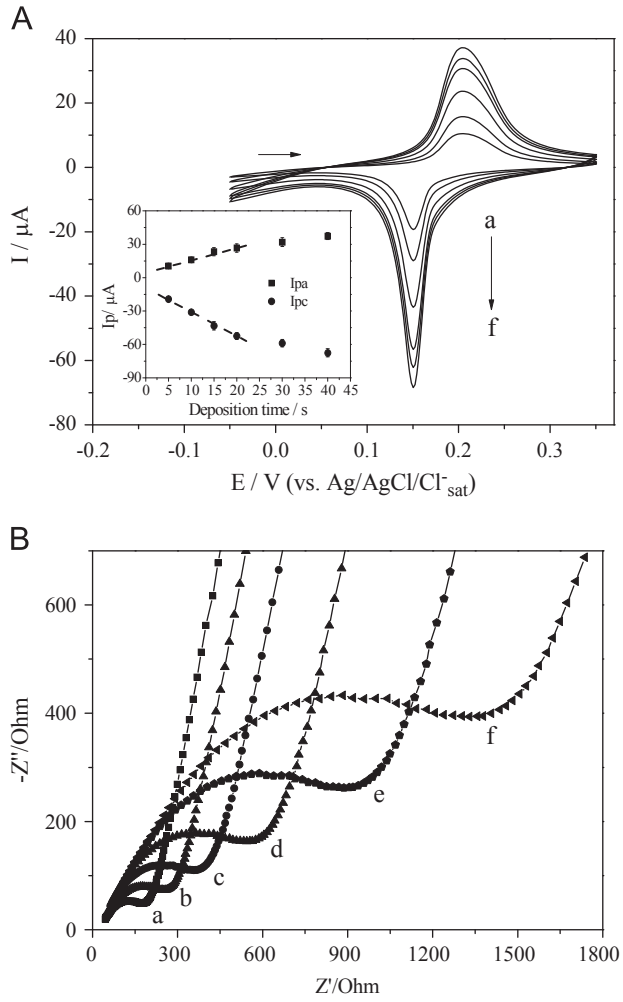

Fig. 2. (A) Cyclic voltammograms of electrodeposited Prussian blue films on GPE using an electrodeposition potential of 0.4 V during (a) 5, (b) 10, (c) 15, (d) 20, (e) 30 and (f) 40 s in 0.1 mol L^{-1} KCl and 0.1 mol L^{-1} HCl at 40 mV s^{-1}. (B) Nyquist plots of electrodeposited Prussian blue films on GPE during (a) 5, (b) 10, (c) 15, (d) 20, (e) 30 and (f) 40 s, for a frequency range of 10^5–10^{-1} Hz. Experimental conditions: 0.04 mol L^{-1} Britton–Robinson buffer (pH 5), 4.75×10^{-5} mol L^{-1} 4-AMP as redox mediator, and 0.2 V of conditioning potential.

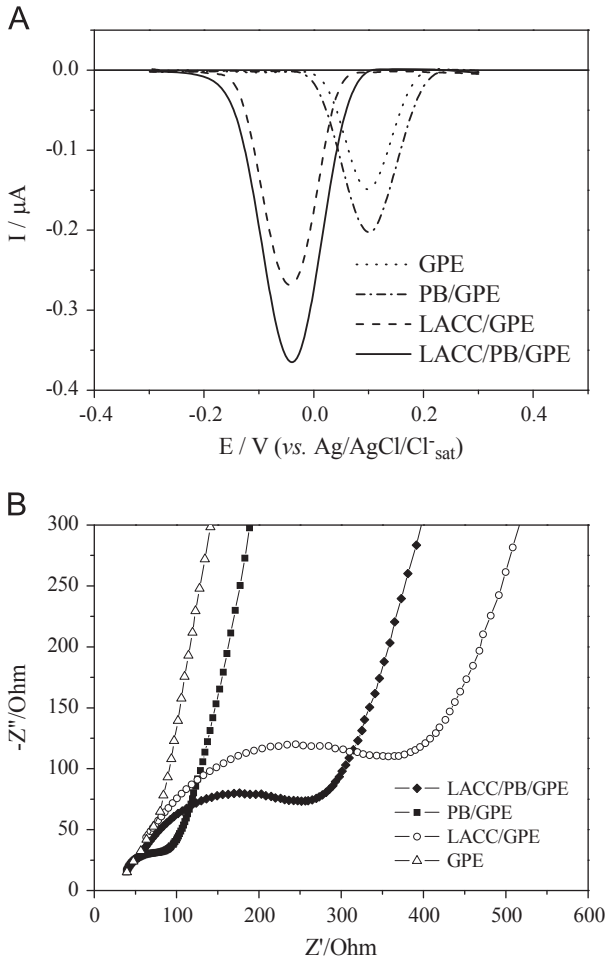

Fig. 3. (A) Square-wave voltammograms of 4.75×10^{-5} mol L^{-1} 4-AMP (0.04 mol L^{-1} Britton–Robinson buffer, pH 5) obtained with (dotted line) bare GPE, (dotted and dashed line) PB/GPE, (dashed line) LACC/GPE, and (solid line) LACC/PB/GPE. Square-wave voltammetric conditions: frequency 100 s^{-1}, pulse amplitude 50 mV and scan increment 2 mV. (B) Nyquist plots of electrochemical impedance spectroscopy for bare GPE, PB/GPE, LACC/GPE, and LACC/PB/GPE in 4.75×10^{-5} mol L^{-1} 4-AMP (0.04 mol L^{-1} Britton–Robinson buffer, pH 5) for a frequency range of 10^5–10^{-1} Hz, applying 0.20 (in the absence of LACC) and −0.01 V (in the presence of LACC).

3.2.3. *Immobilization of LACC onto the Prussian blue film–graphene doped carbon paste modified electrode*

In neutral and basic pH, PB films have the drawback of being highly soluble, thus the use of polymeric films (Nafion, polypyrrol, polyaniline or chitosan) coated over PB layers is mandatory (Jiang et al., 2011; Bo et al., 2011). However, in acidic conditions, PB films are not disrupted and exhibit good stability. It was verified that the use of specific reagents to cross-link LACC and PB/GPE was not necessary. Thus, LACC was immobilized directly on PB film by drop coating to enhance the electron transfer of the redox process and the catalytic effect of the enzymatic biosensor in relation to the 4-AMP substrate. This procedure also facilitates the construction of the device and makes it faster and less expensive. Fig. 3A presents the square-wave voltammograms for 4-AMP reduction processes on GPE, PB/GPE, LACC/GPE and LACC/PB/GPE, in 0.04 mol L^{-1} Britton–Robinson, after 30 min incubation time. In the absence of LACC, the reduction process of 4-AMP occurred at +0.10 V. The quinone–imine intermediate easily hydrolyzes to *p*-quinone in acid conditions (Salavagione et al., 2004; Oliveira et al., 2013). Thus, when LACC is immobilized on the electrode surface, the imine–quinone reduction reaction is catalyzed, and a new process related to reduction of *p*-quinone is observed at −0.05 V which was used as the analytical signal. Although LACC/GPE exhibited a good catalytic effect, the intensity of peak current obtained with LACC/PB/GPE was clearly higher (*ca.* 27%).

The LACC stability on the GPE and PB/GPE was also evaluated by fifty consecutive cyclic voltammograms in 4-AMP (30 min of incubation time before the first scan). A 28% decrease in the analytical signal current was observed for LACC/GPE, while LACC/PB/GPE proved to be more stable with a variation of just 7.0%. The Nyquist plots presented at Fig. 3B also show that the immobilization of LACC on the electrode surface by drop coating promoted the increase of the capacitance of the device, but this effect is lower for LACC/PB/GPE (R_{et}=267 Ω) than for LACC/GPE (R_{et}=396 Ω), highlighting the importance of electrodeposited PB in the conductibility of the composite material. The increase in the capacitance arc also confirms the success of the enzyme immobilization step on GPE and PB/GPE surfaces. These data show that the LACC/PB/GPE configuration is more suitable as a biosensor.

3.3. *Optimization of the LACC/PB/GPE experimental parameters*

Optimization of the operational conditions was carried out by a 2^3 full-factorial statistical design and RSM, in order to evaluate the

combined effect of the pH (X_1), enzyme concentration (X_2) and incubation time (X_3) on the biosensor performance (Fig. 4A, C). Optimum conditions were obtained through close observation of experimental data, inspection of 3D surface plots, and based on ANOVA results (Montgomery, 2005).

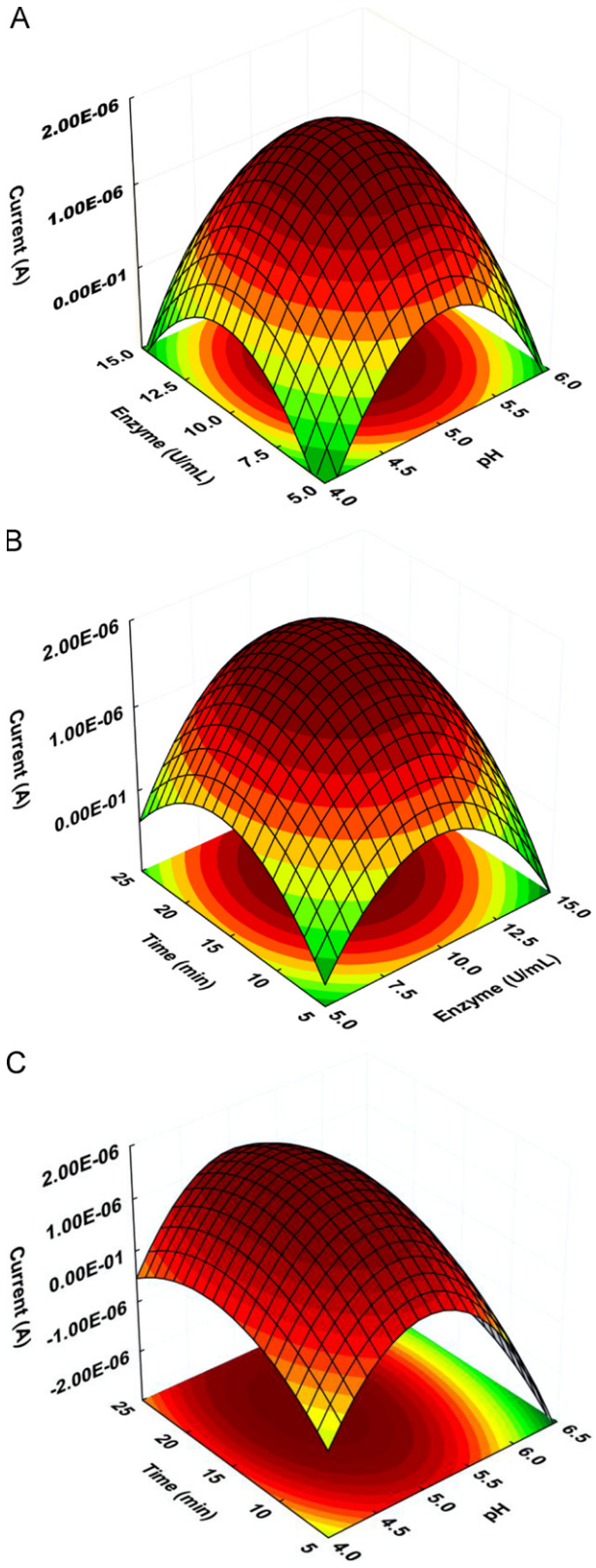

Fig. 4. Response surface plots of the intensity of 4.75×10^{-5} mol L^{-1} 4-AMP peak current as a function of: (A) pH and enzyme concentration (deposition time of 15 min.), (B) enzyme concentration and deposition time (pH 5), and (C) pH and deposition time (enzyme concentration of 10 U mL^{-1}).

The coefficients of the coded regression model were determined based on the experimental results presented in Table 1. By eliminating the non-significant parameters ($p > 0.05$), response surface regression originated the following second-order model:

$$Y = -4.67 \times 10^{-5} + 1.64 \times 10^{-5} x_1 - 1.64 \times 10^{-6} x_1^2 - 5.06 \times 10^{-8} x_2^2 + 2.64 \times 10^{-7} x_3 - 9.36 \times 10^{-9} x_3^2 \quad (2)$$

Table 1 summarizes the experimental and predicted responses, as well as the analysis of variance (ANOVA) for the regression model. The adequacy and significance of the quadratic model was verified by Fisher's F test; the obtained F value (6.102) at a low probability ($p < 0.05$) indicates appropriate significance of the model. However, some lack of fit persisted. This apparent contradiction may be due to the limited number of experimental observations used to produce an appropriate analysis of the residues and because of the number of parameters studied (Montgomery, 2005). Still, the attained R^2 (0.8086) is clearly acceptable for data of a chemical nature (Sousa et al., 2012; Montgomery, 2005) indicating that the biosensor response is adequately fitted by the developed model. A good correlation between observed and predicted values was verified. According to ANOVA results concerning interaction and quadratic effects (results not shown), the principal influencing parameters are, in descending order, $X_1^2 (p < 0.0001)$, $X_2^2 (p < 0.001)$ and $X_3^2 (p < 0.01)$ probably because the enzyme activity is strongly pH- and concentration-dependent. The obtained convex response surfaces (Fig. 4A–C) indicated that the biosensor response increased with the increase in pH, enzyme concentration and incubation time up to the critical values: pH 5.0, enzyme concentration of 10.2 U mL^{-1} and incubation time of 17.2 min. Testing these conditions and those of the central point with the student's t-test ($n = 6$, five degrees of freedom, and 95% confidence level) the responses attained were not statistically different. Considering time savings and the method throughput, the selected optimum conditions were pH 5.0, enzyme concentration of 10 U mL^{-1}, and 15 min of incubation time.

SWV parameters (frequency 10–300 Hz, amplitude 10–60 mV and step 1–8 mV) were also optimized based on I_p intensity, displacement of E_p and increase of $\Delta E_{p/2}$. The best results were attained for 100 Hz, 40 mV and 3 mV, which were applied to subsequent analyses.

3.4. Carbamate pesticides quantification

Trace concentrations of the selected carbamates were determined by inhibition of the reduction process of p-quinone to hydroquinone registered at −0.05 V. Carbamates calibration data are summarized in Table 2. All analytical curves presented acceptable linearity and low dispersion of the data at low concentrations (Fig. 1S, supplementary material) with correlation coefficients (r) ranging from 0.9989 to 0.9997. The standard deviation of the intercepts and the average of slopes of the straight lines from the analytical curves were used to determine the detection (LOD) and quantification limits (LOQ) (Miller and Miller, 2005). The highest sensitivity was attained for CBR (LOD 5.5×10^{-9} mol L^{-1}; 0.001 mg kg^{-1} w/w) and ZRM (LOD 5.2×10^{-9} mol L^{-1}; 0.002 mg kg^{-1} w/w) which promoted the strongest inhibition of the enzyme activity. Regarding the other pesticides, acceptable results were also obtained with LOD values ranging from 3.1×10^{-8} mol L^{-1} (0.007 mg kg^{-1} w/w; PMB) to 1.0×10^{-7} mol L^{-1} (0.022 mg kg^{-1}; CBF). The sensitivity of the proposed methodology is sufficient to enable testing of compliance with food regulations and established maximum residue levels (0.1 to 3.0 mg kg^{-1} for tomato and 0.05 to 0.1 mg kg^{-1} for potato) for all carbamates tested (EU pesticide residues database, 2012; ANVISA, 2012).

Table 2
Carbamate pesticides calibration and recovery data obtained with the optimized LACC/PB/GPE in QuEChERS vegetable extracts. Square-wave voltammetric conditions: 4.75×10^{-5} mol L^{-1} 4-AMP (0.04 mol L^{-1} Britton–Robinson buffer, pH 5), frequency 100 s^{-1}, pulse amplitude 40 mV and scan increment 3 mV.

Calibration data	Carbamate pesticide [a]				
	CBF	CBR	FMT	PMB	ZRM
Linear range (mol L^{-1})	4.98×10^{-7} to 5.88×10^{-6}	7.44×10^{-8} to 8.47×10^{-7}	2.49×10^{-7} to 4.76×10^{-6}	2.99×10^{-7} to 5.66×10^{-6}	2.49×10^{-8} to 5.66×10^{-7}
Intercept (% inhibition)	0.50	1.69	0.16	5.95	3.40
SD_a [b]	0.12	0.30	0.01	0.22	0.35
Slope (% inhibition mol^{-1} L)	3.53×10^6	1.66×10^8	5.94×10^5	2.16×10^7	2.02×10^8
SD_b [c]	1.10×10^4	1.61×10^6	2.95×10^4	2.08×10^4	1.15×10^5
r	0.9993	0.9989	0.9992	0.9997	0.9993
LOD (mg kg^{-1})	0.022	0.001	0.013	0.007	0.002
LOQ (mg kg^{-1})	0.074	0.003	0.045	0.024	0.006
Repeatability [d] (intra-day, %)	2.1	3.3	2.9	2.5	1.8
Repeatability [d] (inter-day, %)	3.4	3.8	3.4	2.9	2.4
Reproducibility (%)	6.3	4.8	4.1	4.9	5.0
Spiking assays in vegetable extracts					
Spiking level I (mg kg^{-1})	0.21	0.02	0.21	0.23	0.02
Recovery in tomato (%)	90.2 ± 0.1	92.7 ± 0.4	94.6 ± 0.1	96.9 ± 0.1	97.6 ± 0.1
Recovery in potato (%)	94.0 ± 0.3	95.0 ± 0.4	91.0 ± 0.1	97.0 ± 0.1	98.0 ± 0.1
Spiking level II (mg kg^{-1})	0.54	0.06	0.64	0.58	0.10
Recovery in tomato (%)	95.8 ± 0.1	97.5 ± 0.5	97.1 ± 0.3	100.3 ± 0.2	101.1 ± 0.3
Recovery in potato (%)	96.1 ± 0.2	97.7 ± 0.4	95.8 ± 0.1	98.5 ± 0.1	100.8 ± 0.1

[a] CBF—carbofuran; CBR- carbaryl; FMT- formetanate; PMB- pirimicarb; ZRM- ziram;
[b] SD_a—Standard deviation of the intercept;
[c] SD_b—Standard deviation of the slope;
[d] Relative standard deviations of 10 pesticide determinations at 1.96×10^{-7} mol L^{-1} for CBR and ZRM, and 1.96×10^{-6} mol L^{-1} for CBF, FMT and PMB.

The intra- and inter-day repeatability of the proposed electroanalytical protocol was also evaluated by the relative standard deviations (RSD). RSD values ranged from 1.8 to 3.3% for intra-day repeatability, and 2.4 to 3.8% for inter-day repeatability (Table 2). The reproducibility assays were also made through the comparison of the RSD values of responses obtained by four different LACC/PB/GPE biosensors to the same conditions previously described; the obtained values varied between 4.1 and 6.3%. The stability of the biosensor was also evaluated and the high activity and catalytic properties of the enzyme were retained over a period of twenty days; the device retained 90.5% of its initial current response. Overall, it can be concluded that the developed LACC/PB/GPE biosensor exhibits relevant advantages (easy preparation, good stability, acceptable repeatability and reproducibility, and relatively short time of analysis) for carbamate analysis.

3.5. Application to vegetable samples

QuEChERS (Paíga et al., 2012; Anastassiades et al., 2003) extraction method was applied with the LACC/PB/GPE at optimal operational conditions to tomato and potato samples. The accuracy of the proposed electroanalytical protocol was evaluated by recovery assays preformed at two spiking levels by the standard additions method (Table 2). Acceptable recoveries (from $90.2 \pm 0.1\%$ to $101.1 \pm 0.3\%$ for tomato, and from $91.0 \pm 0.1\%$ to $100.8 \pm 0.1\%$ for potato samples) were attained. These values compare favorably with those reached by previously reported acetylcholinesterase and cholinesterase-based biosensors for CBR (Caetano and Machado, 2008; Bucur et al. 2006; Nunes et al., 1999), CBF and PMB (Bucur et al. 2006).

Considering that tomato and potato are important sources of β-carotene (pro-vitamin A), thiamine (vitamin B1) and ascorbic acid (vitamin C), these compounds were tested as possible interferences in the analytical response of the developed biosensor (results not shown). SWV assays were carried out at optimal conditions in the presence of interference/substrate ratios of 1:10, 1:1 and 10:1 (w/w), and the results expressed as bias (%). Vitamin B1 showed no significant effect (a signal reduction of $5.3 \pm 0.1\%$ at the higher ratio tested). However, higher bias were detected for pro-vitamin A ($11.4 \pm 0.1\%$) and vitamin C ($13.2 \pm 0.2\%$) at the maximum ratio level. Bearing in mind that the highest ratio tested corresponds to an extreme condition which is seldom found in a 10 g mass of the analyzed vegetables, these results confirm the acceptable selectivity and accuracy of the pesticide residues methodology proposed herein.

4. Conclusions

Graphene doped carbon paste and LACC present interesting electrochemical and catalytic properties for the development of enzymatic biosensors, and that PB films allow the direct immobilization of LACC in acidic conditions, without the use of any cross-linking agent. Moreover, the electrodeposited PB film significantly decreases the R_{et} of the transducer, even after LACC immobilization. The combined effects of the pH, LACC concentration and incubation time were optimized by a 2^3 full-factorial and RSM, with good agreement between the predicted and experimental signals. Considering that studies dealing with practical applications of enzymatic biosensors using food samples are limited, the electroanalytical performance of the developed device in vegetable crops was also evaluated. The developed LACC/PB/GPE exhibited suitable sensitivity, repeatability, reproducibility, selectivity, accuracy and stability (*ca.* twenty days) for the quantification of CBF, CBR, FMT, PMB and ZRM which are widely applied on tomato and potato crops, The combination of these advantages with the efficiency of the QuEChERS extraction method enables the biosensing of the selected carbamate residues and its implementation in food safety programs.

Acknowledgements

The authors thank CAPES and FCT for the financial support through the project (No. 313/11), and FCT through the project

PEst-C/EQB/LA0006/2011. M. F. Barroso is grateful to FCT for her post-doc fellowship SFRH/BPD/78845/2011.

Appendix A. Supporting information

Supplementary data associated with this article can be found in the online version at http://dx.doi.org/10.1016/j.bios.2013.03.026.

References

Anastassiades, M., Lehotay, S.J., Stajnbaher, D., Schenck, F.J., 2003. Journal of AOAC International 86, 412–431.

ANVISA (Agência Nacional de Vigilância Sanitária, Brasil). Monographs of authorized pesticides. Accessed from ⟨http://portal.anvisa.gov.br/wps/content/Anvisa+Portal/Anvisa/Inicio/Agrotoxicos+e+Toxicologia/Assuntos+de+Interesse/Monografias+de+Agrotoxicos/Monografias⟩ (September 2012).

Bo, Y., Wang, W., Qi, J., Huang, S., 2011. Analyst 136, 1946–1951.

Bucur, B., Fournier, D., Danet, A., Marty, J.-L., 2006. Analytica Chimica Acta 562, 115–121.

Caetano, J., Machado, S.A.S., 2008. Sensors and Actuators B 129, 40–46.

Durán, N., Rosa, M.A., D'Annibale, A., Gianfreda, L., 2002. Enzyme and Microbial Technology 31, 907–931.

Dyk, J.S.V., Pletschke, B., 2011. Chemosphere 82, 291–307.

EU pesticide residues database. EU pesticide residues database for all the EU-MRLs. Available from ⟨http://ec.europa.eu/food/plant/protection/pesticides/database⟩ (October 2012).

European Council Directive 2002/63/CE. Establishing Community methods of sampling for the official control of pesticide residues in and on products of plant and animal origin and repealing Directive 79/700/EEC.Official Journal of the European Communities, L187/30-31.

Fu, G., Yue, X., Dai, Z., 2011. Biosensors and Bioelectronics 26, 3973–3976.

Gu, H., Yu, Y., Liu, X., Ni, B., Zhou, T., Shi, G., 2012. Biosensors and Bioelectronics 32, 118–126.

Jiang, Y., Zhang, X., Shan, C., Hua, S., Zhang, Q., Bai, X., Dan, L., Niu, L., 2011. Talanta 85, 76–81.

Khan, U., Porwal, H., O'Neill, A., Nawaz, K., May, P., Coleman, J.N., 2011. Langmuir 27, 9077-9082.

Kondapalli, S.P., Chalamalasetti, S.R., Damera, N.R., 2012. Journal for Manufacturing Science and Production 12, 17–24.

Kuila, T., Bose, S., Khanra, P., Mishra, A.K., Kim, N.H., Lee, J.H., 2011. Biosensors and Bioelectronics 26, 4637–4648.

Li, L., Sheng, Q., Zheng, J., Zhang., H., 2008. Bioelectrochemistry 74, 170–175.

Maia, F.J.N., Clemente, C.S., Oliveira, T.M.B.F., Lomonaco, D., Oliveira, T.I.S., Almeida, M.O., De Lima-Neto, P., Correia, A.N., Mazzeto, S.E., 2012. Electrochimica Acta 79, 67–73.

Miller, J.N., Miller, J.C., 2005. Statistics and chemometrics for analytical chemistry. Pearson Prentice Hall, United Kingdom.

Montgomery, D.C., 2005. Design and analysis of experiments, 6th ed. John Wiley & Sons, Inc., USA.

Morozova, O.V., Shumakovich, G.P., Shleev, S.V., Yaropolov, Y.I., 2007. Applied Biochemistry and Microbiology 43, 523–535.

Novoselov, K.S., Geim, A.K., Morozov, S.V., 2004. Science 306, 666–669.

Nunes, G.S., Barceló, D., Grabaric, B.S., Díaz-Cruz, J.M., Ribeiro, M.L., 1999. Analytica Chimica Acta 399, 37–49.

Oliveira, T.M.B.F., Becker, H., Longhinotti, E., De Souza, D., De Lima-Neto,P.,Correia, A. N., Microchemical Journal, 2012, http://dx.doi.org/10.1016/j.microc.2012.03.032, in press.

Oliveira, T.M.B.F., Barroso, M.F, Morais, S., De Lima-Neto, P., Correia, A.N., Oliveira, M. B.P.P., Delerue-Matos, C., 2013. Talanta 106, 137–143.

Paíga, P., Morais, S., Oliva-Teles, T., Correia, M., Delerue-Matos, C., Duarte, S.C., Pena, A., Lino, C.M., 2012. Food Chemistry 135, 2522–2528.

Pumera, M., Ambrosi, A., Bonanni, A., Chng, E.L.K., Poh, H.L., 2010. TRAC, Trends in Analytical Chemistry 29, 954–965.

Ricci, F., Palleschi, G., 2005. Biosensors and Bioelectronics 21, 389–407.

Sabela, M.I., Gumede, N.J., Singh, P., Bisetty, K., 2012. International Journal of Electrochemcal Science 7, 4918–4928.

Salavagione, H.J., Arias, J., Garcés, P., Morallón, E., Barbero, C., Vázquez, J.L., 2004. Journal of Electroanalytical Chemistry 565, 375–383.

Schulte-Oehlmann, U., Oehlmann, J., Keil, F., 2011. Reviews of Environmental Contamination and Toxicology 213, 137–159.

Schwarzenbach, R.P., Escher, B.I., Fenner, K., Hofstetter, T.B., Johnson, C.A., von Gunten, U., Wehrli, B., 2006. Science 313, 1072–1077.

Shao, Y., Wang, J., Wu, H., Liu, J., Aksay, I.A., Lin, Y., 2010. Electroanalysis 22, 1027–1036.

Sousa, A.M.M., Morais, S., Abreu, M.H., Pereira, R., Sousa-Pinto, I., Cabrita, E.J., Delerue-Matos, C., Gonçalves, M.P., 2012. Journal of Agricultural and Food Chemistry 60, 4977–4985.

USEPA (United States Environmental Protection Agency), 2012a. National Survey of Pesticides in Drinking Water Wells, Phase II Report, EPA 570/8-91-020, National Technical Information Service. Springfield, VA.

USEPA (United States Environmental Protection Agency). Regulating pesticides. Accessed from ⟨http://www.epa.gov/pesticides/regulating/index.htm⟩ (September 2012b).

Xue, M.-H., Xu, Q., Zhou, M., Zhu, J.-J., 2006. Electrochemistry Communications 8, 1468–1474.